In Vivo Bone Strain and Ontogenetic Growth Patterns in Relation to Life-History Strategies and Performance in Two Vertebrate Taxa: Goats and Emu*

Russell P. Main†
Andrew A. Biewener
Concord Field Station, Department of Organismic and Evolutionary Biology, Harvard University, 100 Old Causeway Road, Bedford, Massachusetts 01730

Accepted 12/13/2004; Electronically Published 11/16/2005

ABSTRACT

This study examined ontogenetic patterns of limb loading, bone strains, and relative changes in bone geometry to explore the relationship between in vivo mechanics and size-related changes in the limb skeleton of two vertebrate taxa. Despite maintaining similar relative limb loads during ontogeny, bone strain magnitudes in the goat radius and emu tibiotarsus generally increased. However, while the strain increases in the emu tibiotarsus were mostly insignificant, strains within the radii of adult goats were two to four times greater than in young goats. The disparity between ontogenetic strain increases in these taxa resulted from differences in ontogenetic scaling patterns of the cross-sectional bone geometry. While the cross-sectional and second moments of area scaled with negative allometry in the goat radius, these measures were not significantly different from isometry in the emu tibiotarsus. Although the juveniles of both taxa exhibited lower strains and higher safety factors than the adults, the radii of the young goats were more robust relative to the adult goats than were the tibiotarsi of the young compared with adult emu. Differences in ontogenetic growth and strain patterns in the limb bones examined likely result from different threat avoidance strategies and selection pressures in the juveniles of these two taxa.

* This article was presented at the symposium "The Ontogeny of Performance in Vertebrates," Seventh International Congress of Vertebrate Morphology, Boca Raton, Florida, 2004.

† Corresponding author; e-mail: rmain@oeb.harvard.edu.

Physiological and Biochemical Zoology 79(1):57–72. 2006. 1522-2152/2006/7901-4151$15.00

Introduction

Vertebrates vary in size both through ontogeny and across phylogenetically different taxa. Phylogenetic differences in size are clearly most extreme, with terrestrial vertebrates spanning a six order of magnitude difference in body mass (Alexander et al. 1979). Although the potential size range within a single taxon is much less than across taxa, terrestrial vertebrates show a smaller but still significant increase in mass (10× to 40×) during ontogenetic growth (Garland 1985; Biewener et al. 1986; Brear et al. 1990; Carrier and Leon 1990). Interestingly, in the taxa examined to date, peak locomotor limb bone strains or stresses are remarkably similar in adults despite the size range and diversity of forms examined, which include, among others, horses, dogs, macaques, chipmunks, and alligators (Rubin and Lanyon 1982; Biewener et al. 1983; Biewener 1991; Blob and Biewener 1999; Demes et al. 2001). Although these forms are diverse in their musculoskeletal organization, modifications in three main aspects of the skeletal support system are able to accommodate the observed size range without substantial loss of performance: (1) the material properties of the bones, (2) bone shape or geometry, and (3) posture, which may decrease bone and muscle stresses in larger animals by generally increasing the effective mechanical advantage of their musculoskeletal systems (Biewener 1989). At very large sizes, however, simply altering these three features is not enough to allow the limb skeleton to withstand the increase in mass, and certain aspects of locomotor performance inevitably decrease (Biewener 1982, 1983, 1989).

The elastic modulus (E) of a material indicates its stiffness, or resistance to deformation when subjected to a load (Currey 2002), and is defined as the relative change in length of the material ($\Delta l/l$; strain, ε) for an applied stress ($\mathbf{F}/A$, where $\mathbf{F}$ is the applied force and A is the material area over which $\mathbf{F}$ is applied). In bone, a greater elastic modulus generally results from increased mineral content (Currey 1999). Across vertebrates, the elastic modulus and ultimate strength of the appendicular long bones are not significantly different (Biewener 1982; Currey 1987; Erickson et al. 2002). However, this is not the case through ontogeny, where bone mineralization and consequently elastic modulus increase as animals grow and mature (Currey and Pond 1989; Brear et al. 1990; Currey 1999). So, whereas only bone shape and posture appear to be modulated across adult taxa to accommodate interspecific increases in size,

ontogenetic increases in size are additionally compensated for by an increase in the mechanical stiffness of the bone material.

Both cross-sectional bone geometry and bone curvature affect how forces are transmitted through the limb and the resulting deformations of the limb bones. Straighter bones, similar to straighter limbs in general, transmit locomotor and gravitational forces in a more axial manner than bones with greater longitudinal curvatures, which induce bending moments in the midshaft region of a bone. A given force applied to the end of a bone will result in much greater deformation if it induces bending rather than a purely axial load on the bone's shaft. Thus, larger mammals generally have relatively straighter limb bones than smaller mammals to decrease the relative amount of bending to which their bones are subjected (Bertram and Biewener 1992). This is not true in birds, however, because larger avian taxa actually have more curved limb bones than small ones (Cubo et al. 1999). In the only study in which they have been examined, ontogenetic changes in bone curvature were found to be insignificant in the chicken tibiotarsus (Tbt; Biewener and Bertram 1994).

The cross-sectional area (A), second moments of area (I), and polar moment of inertia (J) are measurements of bone geometry that indicate a bone's ability to resist the axial, bending, and torsional forces transmitted through the bone, respectively. Bone cross-sectional area has been found to increase relative to body mass (positive allometry) across taxa of various sizes (Biewener 1982; Cubo and Casinos 1998; Polk et al. 2000) but to decrease relative to ontogenetic increases in mass (negative allometry; Biewener and Bertram 1994). Similarly, the second moment of area (I) has generally been found to increase (slight positive allometry; Biewener 1982) or remain similar (isometry; Cubo and Casinos 1998) across increasingly larger taxa and to decrease (negative allometry) or remain similar (isometry) relative to body mass through ontogeny (Carrier 1983; Biewener and Bertram 1994). The polar moment of inertia (J) scales with isometry or positive allometry with an interspecific increase in mass (Selker and Carter 1989; Cubo and Casinos 1998; Polk et al. 2000) but has been suggested to scale with negative allometry during ontogeny in muskoxen (Heinrich et al. 1999).

On the basis of the results of these studies, it appears that the growing vertebrate skeleton employs different strategies (isometry or negative allometry) to accommodate ontogenetic increases in mass than those observed across a broad size range of adult taxa (isometry or positive allometry), suggesting that stress/strain similarity is not maintained in vertebrates during ontogenetic growth. However, even the interspecific scaling patterns, which generally show only moderate relative increases in cross-sectional geometry, are not sufficient to maintain stress/strain similarity, so alternative strategies are often employed to decrease the mechanical forces experienced by the bones of larger animals.

Postural changes producing a more upright limb orientation in larger vertebrates have been hypothesized to decrease the forces exerted on the limb musculoskeletal system (Biewener 1983, 1989) by aligning the locomotor forces along the long axes of the limb bones, thereby reducing the bending moments on the bones and the muscular forces required to resist moments about the joints. This is consistent with larger animals (horses and ostriches) having more upright or extended limbs than smaller ones (mice and quail; Biewener 1983; Gatesy and Biewener 1991), which maintains stress/strain similarity despite bone diameters and cross-sectional area scaling close to geometric similarity (Alexander et al. 1979; Maloiy et al. 1979; Biewener 1983).

Postural changes have also been observed through ontogeny (Irschick and Jayne 2000) but are generally not as significant as those seen across large size ranges (Biewener 1983; Gatesy and Biewener 1991) or are transient, disappearing very soon after hatching or birth (Muir 2000). These ontogenetic postural changes have also generally been hypothesized to be the result of developing neuromuscular control and coordination (Bradley and Smith 1988; Muir 2000), not necessarily related to size, and the biomechanical effects of such changes have not been examined.

The scaling patterns and behaviors observed in previous studies are useful in that they describe the variety of ways in which the musculoskeletal system compensates for both phylogenetic and ontogenetic increases in size. However, the majority of these studies did not test the significance of their findings by directly measuring in vivo mechanics or performance. The purpose of the work presented here is to link in vivo mechanics with size-related changes in the limb skeleton by examining limb loading, in vivo bone strains, and relative changes in bone geometry through ontogeny in domestic goats and emu.

Emu (*Dromaius novaehollandie*, Mathews, 1910) and domestic goats (*Capra hircus*, Linnaeus, 1758) shared a common ancestor about 320 million years ago (Carroll 1988) whose limb skeleton had to follow certain structural and mechanical rules to resist the gravitational and locomotor forces placed on it. Comparison of these two terminal taxa allows us to address whether these taxa inherited any common solutions to the challenges of supporting an increasing body mass and the associated increasing forces acting on the limb skeleton during ontogenetic growth. The primary reason for focusing on ontogenetic comparisons instead of a broader interspecific approach is that during ontogeny, at least in each of these precocial taxa, posture and musculoskeletal organization are relatively constant across size, which allows us to examine the specific changes in the shape and mineral composition of the bones of the limb skeleton in relation to limb loading and the resulting strains on the bones. By examining the in vivo mechanics and patterns of bone growth through ontogeny, we can address a number of questions. (1) How does the skeleton (both in material and structural properties) accommodate ontogenetic in-

creases in mass? (2) As a result of skeletal ontogenetic growth patterns, are different-sized animals able to maintain similar resistance to mechanical loading and/or similar safety factors? (3) How does the interaction between skeletal growth and increase in body mass affect the animals' behaviors and their responses to selective pressures through ontogeny?

Material and Methods

Similar methods were used for both the goat and emu studies to investigate the relationships between limb loading, in vivo bone strains, and the relative changes in bone geometry through ontogeny in these two taxa. All of the following procedures have been carried out for the goats, since it is a completed and published study (Main and Biewener 2004), but not yet for the emu, since the data presented here are part of an ongoing study. All experimental procedures were approved by the Institutional Animal Care and Use Committee at Harvard University (protocol 21-08).

Ground Reaction Force Data Collection

Ground reaction force (GRF) data were collected to examine how peak limb loads changed through ontogeny with an increase in body weight. They were also recorded before and after the surgery to attach the strain gauges to determine whether GRFs were diminished as a result of any postsurgical lameness. The GRF data were recorded as the animals ran down a runway over a range of gaits and speeds, using a force platform embedded in the runway. The animals were simultaneously filmed from a lateral view to record which limbs made contact with the plate and the timing of foot contact and to ensure that data were analyzed only from trials where the animals were moving at a relatively steady speed.

In comparing limb loading and bone strains through ontogeny, the animals were sampled differently in the two studies. In the goats, animals were divided into three size groups (small, <6 kg; intermediate, 6–11 kg; adult, >15 kg), which also generally separated the animals by age. Two-way ANOVA statistical tests ($P < 0.05$) were used to determine significant differences between limb loading and bone strains in the three groups. The emu were not grouped by age or size. Instead, analyses of limb loading and bone strains were conducted over a continuous range of masses (0.7–36 kg) using least squares regression analyses. Significant trends in the limb loading and bone strain data were determined by 95% confidence intervals (CI) on the least squares regression slopes.

In the goats and emu, the peak vertical and resultant GRFs, respectively, were measured and normalized by the animal's body weight (peak GRF/body weight, **F**/BW) to assess ontogenetic patterns of limb loading. The peak resultant GRF in the emu differed from the peak vertical GRF by only <0.05 **F**/BW, indicating that the vertical component contributed the vast majority of the resultant GRF.

Surgical Procedures and Strain Gauge Attachment

In vivo bone strains were measured from the radius in the goats and from the Tbt in the emu. Because we are interested in exploring general patterns of bone growth and mechanics within the limb skeleton of terrestrial vertebrates during ontogeny, we sampled these two appendicular long bones that, though nonhomologous, both function primarily to resist gravitational forces and transmit locomotor forces to the substrate.

Strain gauges were attached under sterile surgical conditions to the left limb of interest. In the goat radius, sterilized rectangular rosette strain gauges were attached to the cranial (CR) and caudal (CD) midshaft bone surfaces while a single-element strain gauge was attached medially (Fig. 1*A*). Rosette strain gauges are three-element gauges that allow the maximum (tensile) and minimum (compressive) principal strains and their angles (ϕ) relative to the bone's longitudinal axis to be deter-

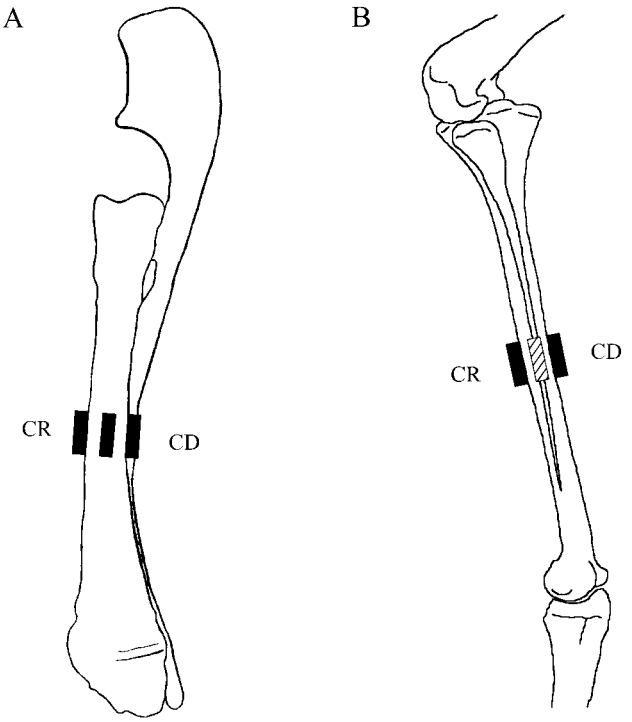

Figure 1. Strain gauge placement for the goat radius and emu Tbt. Illustrations showing the midshaft strain gauge positions of the cranial, caudal, and medial gauges on (*A*) the goat radius (medial view) and (*B*) the emu Tbt (lateral view). The proximal and distal ends of the bones are toward the top and bottom of the figure, respectively. Rosette strain gauges were attached to the cranial and caudal surfaces of the goat radius and to the caudal surface of the emu Tbt. Single-element strain gauges were attached to the medial surface of the radius and to the cranial and medial (hatched) surfaces of the emu Tbt.

mined. In the emu Tbt, a rosette strain gauge was attached to the CD surface of the midshaft of the Tbt, while single-element strain gauges were attached to both the CR and medial (MED) surfaces (Fig. 1*B*).

Strain Data Collection

In vivo bone strain magnitudes and distributions were compared at dynamically similar gaits over the ontogenetic size ranges examined. Dynamic similarity was defined by similar duty factors (DF; Alexander and Jayes 1983), which were measured as the time the animal's foot was in contact with the ground divided by the entire stride time. Comparison of similar gaits based on similar DFs is justified because two animals of different size, moving with the same DF, will have the same relative time, in relation to the stride time, to support their body weight and propel it forward during locomotion. In the goats, dynamic similarity was further defined using distinct gaits characterized by specific footfall patterns.

The animals were given 1–2 d to recover following surgery. If they showed any visible signs of lameness during recovery, an intramuscular injection of analgesic was given every 12 h to relieve soreness in the limb. The goats were run either over ground (small, $N = 4$; intermediate, $N = 6$) or on a motorized treadmill (small, $N = 3$; intermediate, $N = 2$) over a range of speeds and gaits (walk, trot, gallop). Strain data were not collected from adult goats here; instead, strain data from the small and intermediate groups were compared with previously published data from adult goats (Biewener and Taylor 1986). Additionally, because no significant differences in strain magnitude or orientation were found at any site for any gait during treadmill versus over-ground locomotion in the two goats for which equivalent recordings were made (Student's paired *t*-test, $P > 0.05$), data from over-ground and treadmill trials were analyzed together.

All the emu strain data were collected while the animals ($N = 18$) ran on a motorized treadmill over a range of speeds and gaits (walk and run). Terrestrial birds, as opposed to many mammals, do not have distinct gaits that can be defined by characteristic footfall patterns or the presence/absence of an aerial phase (Hildebrand 1965, 1985; Gatesy and Biewener 1991); thus, gait distinctions in the emu were made using center of mass kinematics. From the observed center of mass movements, it was estimated that the emu switched from a walk to a run (or grounded run; Rubenson et al. 2004) at a DF of about 0.60–0.55. This is consistent with previous walk-run transition DFs reported for ostriches and rheas (Gatesy and Biewener 1991; Rubenson et al. 2004). Strain data were collected over a range of DFs from birds walking with a 0.70 DF to birds running with a 0.35 DF. Here, we will focus on comparing data from trials in which the birds were running with a 0.40 DF (0.40 ± 0.01, mean $\pm$ SD), showing a distinct aerial phase. Ontogenetic strain patterns were similar at a walk of 0.65 DF, except the strain magnitudes were typically about 63% of those presented here for a run. After postsurgical in vivo bone strain and GRF data collection was completed, each animal was killed and the relevant limb bones dissected for morphological and histological analysis.

Strain Data Analysis

Data from three to five consecutive foot contacts were chosen from each trial in which the animals moved at a steady pace using a single gait. The raw strain data were analyzed using a custom MATLAB program that zeroed and calibrated the data, converting voltages to microstrain ($\mu\varepsilon$; $\varepsilon \times 10^{-6}$) on the basis of a 1,000-$\mu\varepsilon$ shunt calibration of the bridge amplifier. Zero-strain levels were determined during the swing phase of the limb when the voltage change in the signal was minimal. Principal strains from the rosette strain gauges and strains recorded by the single-element strain gauges were then adjusted to correct for any postsurgical lameness in the limb ($\varepsilon \times [\mathbf{F}/\mathrm{BW}]_{\mathrm{presurgery}}/[\mathbf{F}/\mathrm{BW}]_{\mathrm{postsurgery}}$), assuming that changes in strain are directly proportional to changes in limb loading.

Peak positive (tensile) and negative (compressive) principal strains and their orientations as well as peak tensile and compressive strains from the single-element gauges and the percentage of stance phase when they occurred were determined. In the goat radius, peak axial and bending strains were calculated using the following equations:

$$\varepsilon_{\mathrm{ax}} = \frac{(\varepsilon_{\mathrm{cranial}} + \varepsilon_{\mathrm{caudal}})}{2}. \tag{1}$$

$$\varepsilon_{\mathrm{b}} = \pm \left| \frac{(\varepsilon_{\mathrm{caudal}} - \varepsilon_{\mathrm{cranial}})}{2} \right|. \tag{2}$$

The percentage of total strain in the radius due to bending was calculated as $|\varepsilon_{\mathrm{b}}|/(|\varepsilon_{\mathrm{b}}| + |\varepsilon_{\mathrm{ax}}|) \times 100$.

Bone Geometry and Percentage Mineral Content

Both the cranio-caudal (C-C) and medio-lateral (M-L) curvatures were measured from the noninstrumented (right) limb by dividing the radius of curvature for each direction by half the C-C or M-L diameter of the bone, respectively. The radius of curvature was measured as the orthogonal distance from the C-C or M-L midpoint of the bone at its midshaft to a line bisecting the proximal and distal articular ends of the bone (Bertram and Biewener 1992).

For the goats, the right limb bones were also used to determine the percentage mineral ash content. One-third of the bone's length, centered about the midshaft, was cut and the periosteum and marrow removed and allowed to dry thoroughly. The bone section was weighed and placed in an oven for 12 h at 400°C.

Immediately upon removal from the oven, the ashed bone was weighed again. The percentage mineral ash content was determined as postashed mass/preashed mass × 100.

After measuring the alignment of the strain gauges and their placement relative to the bone's midshaft, the instrumented (left) limb bones were embedded in fiberglass resin and a 60-μm-thick section was taken at the midshaft using a diamond-bladed annular saw. A magnified digital image of the section was taken, and the cross-sectional area, C-C and M-L second moments of area ($I_{C\text{-}C}$ and $I_{M\text{-}L}$, respectively), and the polar moment of inertia were calculated using a custom macro for NIH Image. However, because torsion was not a significant component of the strain patterns observed in the goat radius, the cross-sectional polar moment of inertia for the radius is not presented.

For both taxa, least squares regression analyses were used to examine ontogenetic patterns of bone curvature, cross-sectional geometry, and percentage mineral content versus body mass. Significant trends in the slopes were based on 95% CIs derived from the regressions.

Goat Results

Ontogenetic Changes in Goat Radial Bone Strain

The distribution and alignment of strains in the goat radius were similar in the three size/age groups when moving at similar gaits. At all gaits and speeds, the dominant principal strain on the CR surface was tensile and aligned primarily along the long axis of the bone (Table 1). On the CD surface, the larger principal strain was compressive (Table 1) and, despite greater variability among individuals, was also generally aligned close to the long axis of the bone. Axial strains measured from the MED single-element gauges in the two smaller groups were compressive, while strains on the MED surface were not measured in the previous study for the adult goats (Biewener and Taylor 1986).

Peak strains within the radius increased with an ontogenetic increase in body mass at all gauge locations across the three size/age groups (Fig. 2; Table 1). However, because of high interindividual variation (see Table 3 in Main and Biewener 2004), increases in peak strains within a gait between the small and intermediate groups were significant only on the CR surface ($P < 0.01$; CD, $P = 0.08$; MED, $P = 0.36$). Peak strains in the adult radius, however, were significantly greater than those in the small and intermediate groups (CR and CD, $P < 0.0001$). This is exemplified when strains in the radius are compared at similar absolute speeds in the small and adult groups. At about 2.30 m/s, strains in the radius of the small goats at a gallop were only about 40% of those in the adult goats at a trot (Fig. 2), even though the smaller goats were moving at a relatively faster gait and with a lower DF.

Similar to the increase in principal strains with speed and change of gait, axial and bending strains in the radius also increased in the three groups (Fig. 3). Axial compressive strains increased with speed, although this increase was only significant in the small group (Fig. 3*A*; small: slope, -60.8 ± 22.5, 95% CI, $r^2 = 0.48$; intermediate: -48.6 ± 89.7, $r^2 = 0.04$). Nevertheless, the slopes of the regression lines for the small and intermediate groups were not significantly different from each other (on the basis of their overlapping 95% CI). Strains due to bending did increase significantly in these two groups, but again the slopes of the lines describing these trends did not differ from one another (Fig. 3*B*; small: slope, 241.3 ± 58.8, $r^2 = 0.48$; intermediate: 147.2 ± 53.0, $r^2 = 0.54$).

Table 1: Principal strains and orientation in the goat radius by size group and gait

	Walk		Trot		Gallop	
	$\mu\varepsilon$	ϕ	$\mu\varepsilon$	ϕ	$\mu\varepsilon$	ϕ
Cranial:						
Small	160 ± 125	8 ± 19	267 ± 199	13 ± 14	483 ± 253	−7 ± 19
Intermediate	435 ± 185	12 ± 16	591 ± 249	−2 ± 6	705 ± 302	−7 ± 20
Adult	653 ± 171	4 ± 18	1,192 ± 246	5 ± 13	1,316 ± 79	4 ± 12
Caudal:						
Small	−329 ± 138	18 ± 39	−392 ± 198	15 ± 38	−593 ± 334	16 ± 26
Intermediate	−472 ± 203	−26 ± 38	−654 ± 312	−3 ± 8	−839 ± 457	−1 ± 5
Adult	−850 ± 149	3 ± 14	−1,458 ± 268	−2 ± 14	−1,647 ± 214	−6 ± 12
Medial:						
Small	−516 ± 49		−654 ± 135		−774 ± 329	
Intermediate	−535 ± 268		−802 ± 385		−929 ± 425	

Note. Data for the adult group were calculated from the raw data used in Biewener and Taylor (1986). Values are mean ± SD. Strains from the medial surface are axial compressive strains, not principal strains. $\mu\varepsilon$, microstrain (strain × 10^{-6}); ϕ, orientation, in degrees, of the principal strain relative to the bone's long axis. For the cranial surface, principal strains with a positive ϕ are oriented proximo-medial to disto-lateral relative to the bone's long axis. For the caudal surface, principal strains with a positive ϕ are oriented proximo-lateral to disto-medial relative to the bone's long axis. For sample sizes, see Main and Biewener (2004).

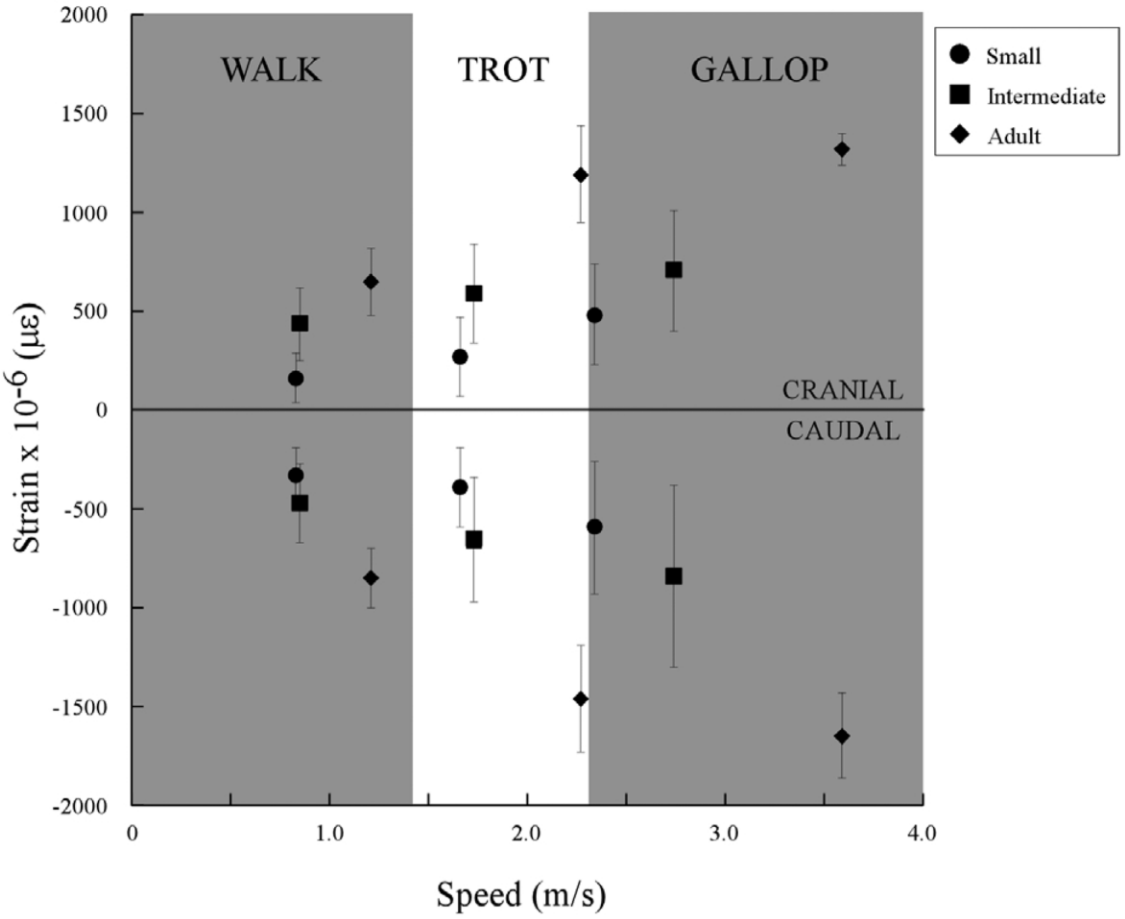

Figure 2. Mean peak principal strain in the goat radius versus mean absolute speed. Mean peak principal tensile and compressive strains from the cranial and caudal surfaces of the goat radius, respectively, plotted versus mean absolute speed for the small, intermediate, and adult groups at a walk, trot, and gallop. Data for the small, intermediate, and adult groups are represented by circles, squares, and diamonds, respectively. Error bars represent ± 1 SD. Error bars for the mean speeds for each age/size group at each gait were omitted for clarity (see Table 1; Main and Biewener 2004).

In all three age/size groups, the major component of strain in the radius midshaft was bending (Fig. 3*C*). This trend remained consistent across speed and gait (regression slopes of percent total strain due to bending were not significantly different from 0; small: 2.4 ± 3.7, $r^2 = 0.05$; intermediate: 2.3 ± 6.5, $r^2 = 0.02$; adult: see Table 1 in Biewener and Taylor 1986). In general, the radius of adult goats experienced the greatest percentage of strain due to bending (mean: 89%; Biewener and Taylor 1986), followed by the small group (73% $\pm$ 9%) and then the intermediate group (70% $\pm$ 18%).

Ontogenetic Changes in Limb Loading

Consistent with the increase in bone strains across speed and gait, normalized vertical GRF exerted on the forelimb also increased (Fig. 4; $P = 0.0001$). However, no significant difference in normalized limb load was observed among the three size classes within each gait ($P = 0.33$). Thus, within a given gait, the radius transmitted limb forces associated with the same relative ground reaction load regardless of size.

Ontogenetic Changes in Radius Cross-Sectional Geometry, Curvature, and Mineralization

Strong patterns of negative allometry were observed in the ontogenetic scaling of the cross-sectional and second moments of area. Midshaft cross-sectional area of the radius scaled proportional to (body mass)$^{0.53 \pm 0.07}$ ($\alpha M^{0.53 \pm 0.07}$, $r^2 = 0.93$; Fig. 5*A*), indicating that the cross-sectional area of the radius became relatively smaller as the animals grew in mass. The midshaft second moments of area in the radius scaled with negative allometry in the M-L ($I_{ML} \alpha M^{1.03 \pm 0.12}$, $r^2 = 0.94$) and C-C

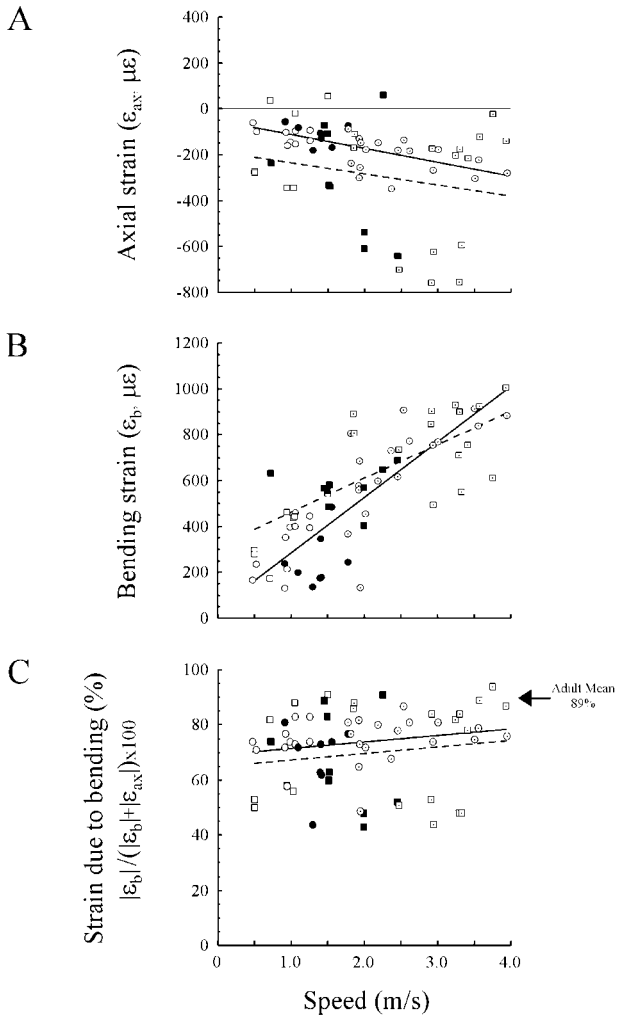

Figure 3. Axial and bending strains and the percent total strain due to bending in the goat radius versus speed. Axial and bending strains in the radius determined from the C-C longitudinal principal strain data based on means for the individual trials at a given speed and gait for all small and intermediate-sized animals. Axial strain (ε_{ax}; *A*), bending strain (ε_b; *B*), and percentage of total strain (*C*) due to bending plotted versus speed. Data for the small and intermediate groups are represented by circles and squares, respectively. Data for walking, trotting, and galloping trials are represented by open, solid, and open with a dot symbols, respectively. The heavy solid regression line is fit to the data for the small group. The dashed line is fit to the data for the intermediate group. *A*, The equations of the regression lines ($\pm$95% CI for the slope, r^2) for the small and intermediate groups are $y = -49.7 - 60.8x$ (± 22.5, $r^2 = 0.48$) and $y = -186.9 - 48.6x$ (± 89.7, $r^2 = 0.04$), respectively. *B*, Small: $y = 44.3 \pm 241.3x$ (± 58.8, $r^2 = 0.68$); intermediate: $y = 312.5 \pm 147.2x$ (± 53.0, $r^2 = 0.54$). *C*, Small: $y = 69.0 \pm 2.4x$ (± 3.7, $r^2 = 0.05$); intermediate: $y = 65.0 \pm 2.3$ (± 6.5, $r^2 = 0.02$). The mean percentage of strain due to bending observed for the adult group is indicated at 89% (Biewener and Taylor 1986). Because of the large variation among individuals within each size/age group, trends for the small and intermediate groups are not significantly different.

($I_{CC} \alpha M^{0.84 \pm 0.16}$, $r^2 = 0.85$) directions (Fig. 5*B*). As a result, the bone's resistance to bending, particularly in the C-C direction, was substantially reduced during growth.

Although cross-sectional geometry showed strong patterns of relative change through ontogenetic growth, there were relatively small changes in both the longitudinal bone curvature and percent mineral content during growth. No significant change in either the C-C or M-L normalized longitudinal bone curvature (C-C, $y = 0.81x^{0.12 \pm 0.14}$, $r^2 = 0.13$; M-L, $y = 0.32x^{0.05 \pm 0.18}$, $r^2 = 0.02$) was observed during ontogeny. As a result, throughout growth, the bone's C-C curvature was consistently greater than its M-L curvature. Similarly, the increase in percentage mineral ash content in the radius, although significant, was small (slope, 0.21 ± 0.07, $r^2 = 0.68$), showing only a 2.8% mean increase from the small to adult groups.

Emu Results

Ontogenetic Changes in Emu Tibiotarsal Strain

Over an ontogenetic increase in mass from 0.7 to 26 kg, the distribution of strains observed on the three bone surfaces at the emu Tbt midshaft during stance was generally consistent at a run of 0.40 DF. Strains measured from the CR Tbt were biphasic with the bone surface being loaded in peak compression 5% $\pm$ 10% of the way through stance and then in peak tension 66% $\pm$ 26% through stance. A similar pattern was observed on the MED Tbt surface, although generally the compressive peak at 28% $\pm$ 5% through stance tended to be higher

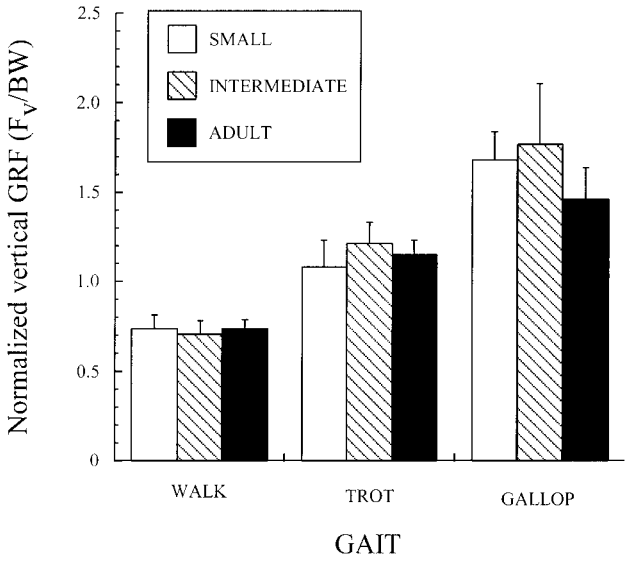

Figure 4. Normalized peak vertical forelimb GRFs versus gait. Normalized peak vertical forelimb GRFs for different gaits in the small, intermediate, and adult groups. Peak vertical forces (F_v) were normalized by dividing the forces by the body weight (*BW*) of the goat. Error bars represent $\pm$1 SD.

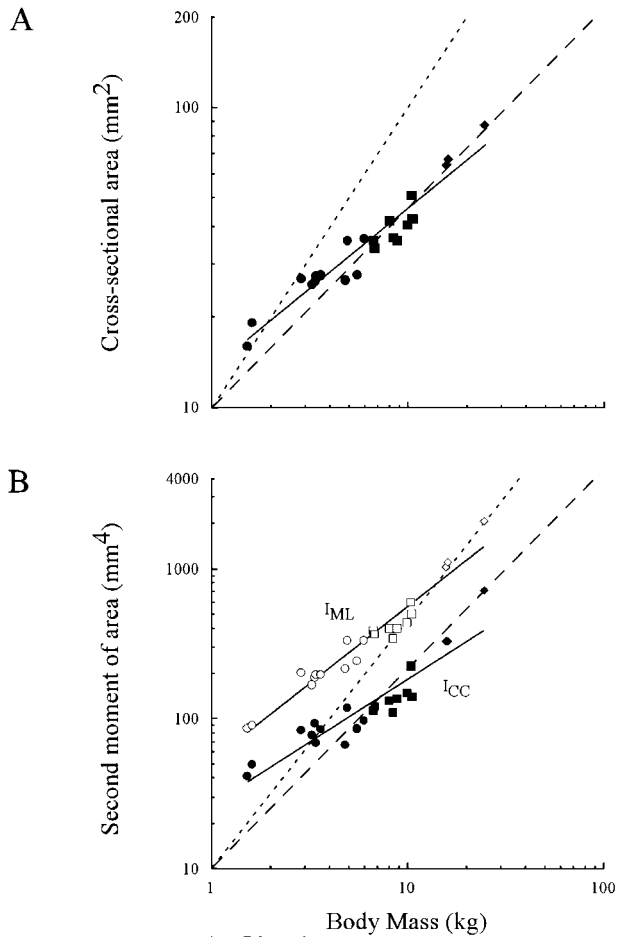

Figure 5. Midshaft cross-sectional bone geometry versus body mass for the goat radius. Cross-sectional area (*A*) and C-C and M-L second moments of area (*B*; *I*) of the goat radius at the midshaft plotted against body mass on logarithmic axes. Data for the small, intermediate, and adult groups are represented by circles, squares, and diamonds, respectively. C-C (I_{CC}) and M-L (I_{ML}) data are represented by closed and open symbols, respectively. *A*, $y = 13.4x^{0.53 \pm 0.07}$ ($r^2 = 0.92$). *B*, I_{CC}: $y = 26.6x^{0.84 \pm 0.16}$ ($r^2 = 0.85$); I_{ML}: $y = 52.3x^{1.03 \pm 0.12}$ ($r^2 = 0.94$). The dashed lines represent isometry in each case (slope: *A*, 0.67; *B*, 1.33), while the dotted lines represent the expected scaling relationships for the maintenance of static strain similarity (slope: *A*, 1.00; B, 1.67). These lines are positioned, starting from the origin, to facilitate comparison with the regression lines (*solid lines*).

than that on the CR surface, and the tensile peak at 96% ± 5% through stance was lower than that on the CR surface. On the CD surface of the Tbt, the larger principal strain was compressive, occurring 43% ± 8% of the way through stance, and was aligned 24° ± 4° proximo-lateral to the long axis of the bone, indicating a degree of torsion on this bone surface. The distribution and orientations of Tbt bone strains through stance were fairly consistent among the emu and are represented for a single 48-wk-old (23 kg) bird in Table 2.

At the similar relative speed of 0.40 DF, peak compressive strains in the Tbt generally increased with an ontogenetic increase in mass, although usually not significantly (Fig. 6). On the CR surface, strains were predominantly compressive in the majority of the birds, especially in those greater than 10 kg (Fig. 6*A*). Although statistically insignificant, peak compressive strains on the CR surface tended to increase during ontogeny (slope, −16.8 ± 19.0, ±95% CI, $r^2 = 0.24$). Peak tensile strains on this same surface remained relatively constant through growth (slope, −2.9 ± 12.4, $r^2 = 0.02$). The MED surface showed similar trends to those on the CR surface, except with generally higher peak compressive strains and lower peak tensile strains than those on the CR surface (Fig. 6*B*). However, unlike the CR surface, the increase in peak compression on the MED Tbt surface was significant (slope, −19.3 ± 17.8, $r^2 = 0.34$), while peak tensile strains again remained relatively constant through ontogeny (slope, 3.2 ± 7.0, $r^2 = 0.09$). Both the peaks in principal tension and compression increased on the CD surface of the Tbt over the size range examined (Fig. 6*C*). However, probably because of a relatively small sample size from the CD strain gauge at this speed, these increases were not significant (slopes: tension, 17.8 ± 18.2, $r^2 = 0.49$; compression, −24.6 ± 26.9, $r^2 = 0.46$).

When comparing strains at a similar absolute speed (mean, 1.07 ± 0.04 m/s; range, 1.01–1.15 m/s), principal strains on the CD Tbt were not significantly different between the smallest and largest (0.7 and 24 kg) emu (Fig. 7). At this speed, "small" emu (<5 kg, 2.4 ± 1.5 kg) moved with a mean DF of 0.61, indicating a fast walk or slow grounded run, while "large" emu (>20 kg, 22.4 ± 2.1 kg) moved with a DF of 0.69, indicating a slow walk. Principal tension remained constant (Fig. 7; slope, 1.1 ± 15.4, $r^2 = 0.003$) at 1.07 m/s. Although principal compression showed a slight increase, the slope of the least squares regression line fit to the data was not significantly different from 0 (Fig. 7; slope, −12.8 ± 20.1, $r^2 = 0.19$). When compared as discrete size groups, the mean peak compressive principal strain for the "small" emu (−457 ± 248 $\mu\varepsilon$, $N = 6$) was not significantly different (Student's paired *t*-test, $P = 0.64$) from the peak strains observed in the "large" emu (−701 ± 182 $\mu\varepsilon$, $N = 3$). Thus, at the same absolute speed, when younger birds are moving at a relatively faster speed (lower DF), they are able to maintain similar, and even somewhat lower, strains to much larger birds moving at relatively slower speeds.

Limb Loading through Ontogeny

There was no significant change during ontogeny in the normalized peak resultant GRF during running (Fig. 8; slope, −0.001 ± 0.01, $r^2 = 0.003$). Thus, when both 2-wk-old and adult emu run, the hindlimb transmits the same relative limb load (2.0 ± 0.2 BW) regardless of size or age. Likewise, the timing and orientation of the peak resultant GRF was similar throughout growth. The peak resultant GRF occurred at 34% ± 8% of the way through stance and was oriented pri-

Table 2: Representative mean tibiotarsus bone strains for a 48-wk-old (23 kg) emu at duty factor 0.40 at six times during stance

	Cranial	Medial	Caudal		
Stance (%)	ε_{ax} ($\mu\varepsilon$)	ε_{ax} ($\mu\varepsilon$)	ε_t ($\mu\varepsilon$)	ε_c ($\mu\varepsilon$)	ϕ
0	−626 ± 3	−170 ± 15	584 ± 114	−187 ± 44	85 ± 0
20	−196 ± 38	−642 ± 103	209 ± 50	−227 ± 143	36 ± 14
40	66 ± 82	−1,160 ± 41	723 ± 9	−883 ± 120	28 ± 4
60	304 ± 40	−645 ± 72	577 ± 3	−909 ± 75	19 ± 4
80	89 ± 106	−61 ± 40	210 ± 34	−368 ± 56	11 ± 3
100	45 ± 31	366 ± 33	78 ± 9	−127 ± 48	63 ± 10

Note. Axial strains (ε_{ax}) for the cranial and medial surfaces, and principal tension (ε_t) and compression (ε_c) for the caudal surface. $\mu\varepsilon$, microstrain (strain × 10^{-6}); ϕ, orientation, in degrees, of ε_c relative to the bone's long axis. ε_t acts normal to ε_c. For the caudal surface, principal strains with a positive ϕ are oriented proximo-lateral to disto-medial relative to the bone's long axis. Values are mean ± SD. $N = 2$ trials (five strides per trial).

marily normal to the point of foot contact at −2° ± 4° in the fore-aft direction (relative to a vertical reference axis) and at 0° ± 2° in the M-L direction.

Ontogenetic Changes in Tbt Cross-Sectional Geometry and Curvature

The results presented here for the scaling patterns of cross-sectional area (A), second moments of area (I), and bone curvature are preliminary, since data from only seven individuals are currently available. However, these data represent nearly the entire size range examined to date (0.90–36 kg). Thus, the patterns of change in cross-sectional bone geometry and curvature reported here are probably representative of patterns that would be produced with a larger sample size, with additional data for intermediate sizes (and ages) relative to the data presented here.

Both emu Tbt cross-sectional area and second moments of area generally scale with isometry during ontogenetic growth. A exhibits some evidence of negative allometry ($\alpha M^{0.62\pm0.07}$, $r^2 = 0.98$; Fig. 9*A*), but this is not significantly different from isometry, indicating that the Tbt maintains nearly the same relative cross-sectional area to support axial loads relative to increases in body mass through growth. Similarly, both I_{CC} and I_{ML}, although showing slight positive growth allometry, do not scale significantly different from isometry ($I_{CC}\alpha M^{1.38\pm0.12}$, $r^2 = 0.99$; $I_{ML}\alpha M^{1.42\pm0.10}$, $r^2 = 0.99$; Fig. 9*B*). Thus, the structural resistance to bending loads in the C-C and M-L directions remains similar relative to body mass in the emu Tbt through growth, with the resistance to bending remaining consistently greater in the M-L plane.

Because the peak principal compression and tension on the CD Tbt, acting at 24° relative to the longitudinal and transverse axes of the Tbt, respectively, indicate significant bone torsion, scaling of the Tbt's polar moment of inertia (J) was also examined. Similar to $I_{ML}$and I_{CC}, J scales with slight positive allometry that is not significantly different from isometry ($\alpha M^{1.40\pm0.11}$, $r^2 = 0.99$; Fig. 9*C*).

Normalized longitudinal bone curvature does not change significantly through ontogeny. Both the MED and CD concave curvatures remain similar through growth (M-L, −0.06 ± 0.19, $r^2 = 0.12$; C-C, −0.17 ± 0.26, $r^2 = 0.34$; Fig. 10), with the M-L curvature generally being larger than that in the C-C direction.

Discussion

Ontogenetic Changes in Bone Loading

In both the goat radius and emu Tbt, bone strains generally increase with an ontogenetic increase in mass. In the goats, radial strains increase significantly through ontogeny from the young goats (4 kg) to the larger adult goats (27 kg) within a given gait and at similar DFs, despite peak limb loads remaining similar through ontogeny at equivalent gaits. In the emu Tbt, only the MED surface of the bone experiences a significant increase in compressive strains through growth. Although both the CR and CD bone surfaces show general increases in peak compressive strains at 0.40 DF, these increases are not significant. However, it is worth noting that this study is ongoing, and the largest bird from which we report strain data here (26 kg) was only 55% of full-grown adult mass.

Although strain magnitudes do not remain consistent through growth, in both species the distribution of compressive and tensile strains within the midshaft of each limb bone and their timing during stance are similarly maintained during ontogeny, as was previously observed within the Tbt of domestic chickens (Biewener et al. 1986). In the goat radius, the CR and CD surfaces consistently develop tensile and compressive peak strains during stance, respectively, indicating that the bone is consistently loaded in C-C bending at all ages/sizes.

The role of bending versus axial compression or torsion has yet to be assessed in the emu Tbt, but the distribution and

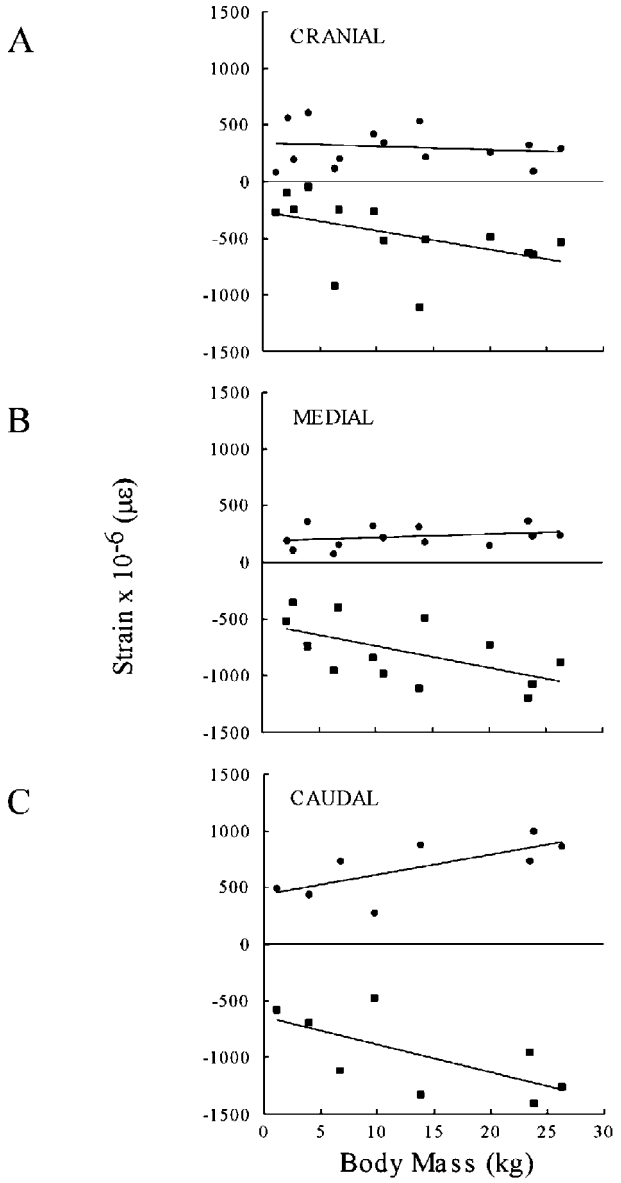

Figure 6. Mean peak bone strain versus body mass for the emu Tbt. Mean peak tensile and compressive axial bone strains from the (*A*) cranial and (*B*) medial surfaces and (*C*) mean peak principal strains from the caudal surface of the emu Tbt plotted against body mass while the birds ran at a DF of 0.40. Tensile and compressive strains are represented by circles and squares, respectively. *A*, The equations for the least squares regression lines for the peak tensile and compressive strains are $y = 338.0 - 2.9x$ (± 12.4, $r^2 = 0.02$) and $y = -268.6 - 16.8x$ (± 19.0, $r^2 = 0.24$), respectively. *B*, Tension: $y = 185.0 \pm 3.2x$ (± 7.0, $r^2 = 0.09$); compression: $y = -544.9 - 19.3x$ (± 17.8, $r^2 = 0.34$). *C*, Principal tension: $y = 435.4 \pm 17.8x$ (± 18.2, $r^2 = 0.49$); principal compression: $y = -639.7 - 24.6x$ (± 26.9, $r^2 = 0.46$). Because multiple trials at this DF were not collected for all birds, for consistency, error bars have been omitted for points that represent a mean of two trials.

timing of peak strains remain fairly consistent through growth, with all three bone surfaces loaded primarily in longitudinal compression, albeit at different times during stance on each surface. The only exception to this trend was observed for the CR surface of the Tbt in birds smaller than 10 kg, in which loading in the bone is more variable, with one-third of the birds under 10 kg showing higher tensile than compressive peak strains. Generally, though, the bones examined in both taxa are loaded in consistent ways across both speed and size.

Because the relative limb loads measured and the observed postures do not change significantly through most of ontogeny in these two taxa, the increased bone strains are likely due to changes in bone cross-sectional geometry, curvature, and/or mineral composition of the bones themselves. Strong negative growth allometry in both the cross-sectional area and second moments of area in the goat radius appears to be primarily responsible for the large increases in strain. Increases in both the axial and bending strains are due specifically to relative decreases in the cross-sectional and second moments of area, respectively. However, in most tetrapod limb bones measured to date, including goats, bending strains are typically the major component of the total strain developed within the midshaft of a bone (Rubin and Lanyon 1982; Biewener and Taylor 1986;

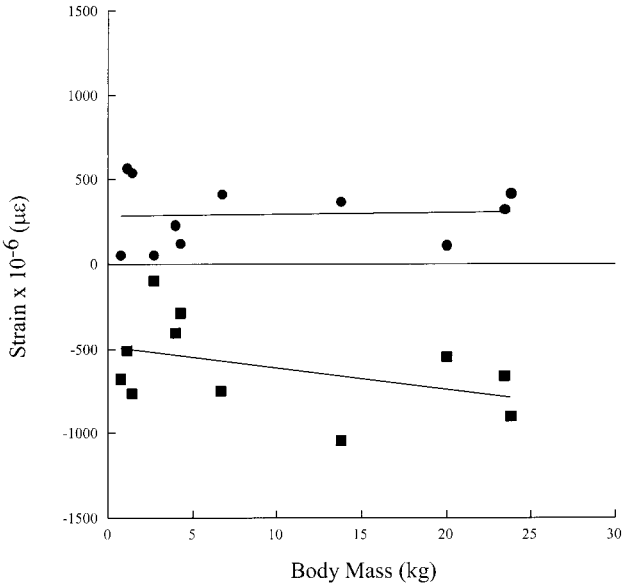

Figure 7. Mean peak bone strains versus body mass for the emu Tbt for birds moving at 1.07 m/s. Mean peak caudal Tbt principal tensile and compressive strains plotted against body mass while the birds moved at an absolute speed of 1.07 m/s (1.07 $\pm$ 0.04, mean $\pm$ SD). Tensile and compressive strains are represented by circles and squares, respectively. Regression slopes: principal tension, $y = 280.7 \pm 1.1x$ (± 15.4, $r^2 = 0.003$); principal compression, $y = -484.3 - 12.8x$ (± 20.1, $r^2 = 0.19$). Because multiple trials at this speed were not collected for all birds, for consistency, error bars have been omitted for points that represent a mean of two trials.

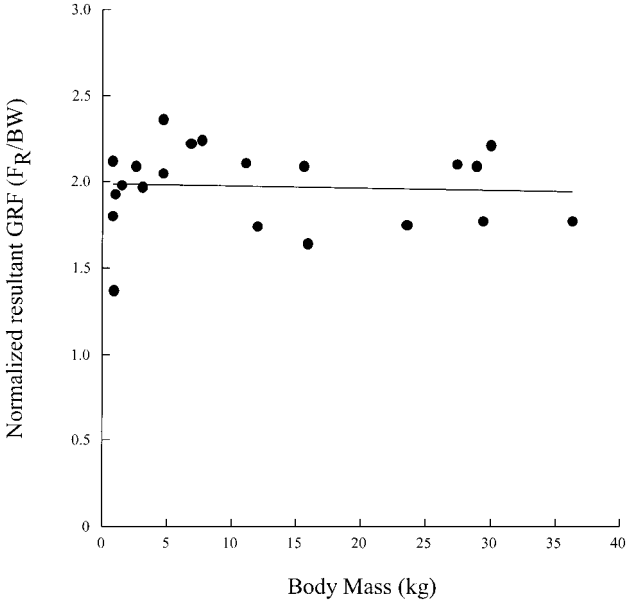

Figure 8. Normalized peak resultant hindlimb GRF versus body mass for running emu. Mean normalized peak resultant hindlimb GRF against body mass for running emu ranging in mass from 0.7 to 36 kg. Peak resultant GRFs (F_R) were normalized by dividing the forces by the body weight (BW) of the emu. Regression slope: $y = 1.99 - 0.001x$ (± 0.01, $r^2 = 0.003$). Error bars have been omitted for clarity.

Biewener 1991). Thus, the strong negative allometry of the second moments of area in the goat radius, which substantially reduced its capacity for resisting bending moments in the C-C and M-L directions, explains most of the increase in locomotor strains as the goats grew in size. Because negative growth allometry in the C-C direction was greater than in the M-L direction, the radius became more eccentric in shape and thus more susceptible to C-C bending as the goats grew. This is consistent with the general increase in strain due to bending found in the C-C direction.

Bone curvature can induce bending moments in bones, thereby increasing (or decreasing, if opposite to external bone bending) the strain due to bending. However, the increases in longitudinal bone curvature in the goat radius through ontogeny were insignificant. Thus, any increase in strain due to greater bone curvature was probably small relative to that produced by the ontogenetic growth patterns in cross-sectional geometry.

Bone mineralization and elastic modulus (E) increase in older animals, with more highly mineralized bone tissue typically having a higher modulus (Currey and Pond 1989; Brear et al. 1990; Currey 1999). Lanyon et al. (1979) observed a 2.1% increase in percent ash content in the sheep radius between 17 wk to >4 yr of age, which corresponded to a 1.27 times increase in E. In the goat radius, we estimated that a 1.77 times increase in E would be necessary to maintain uniform C-C bending

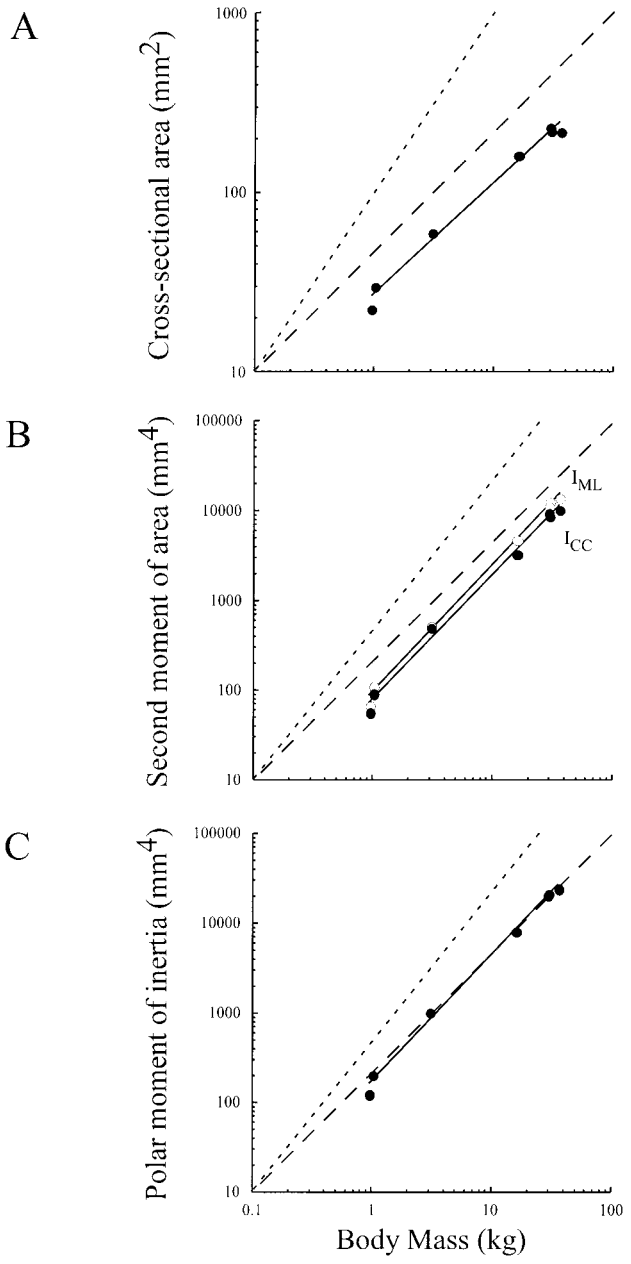

Figure 9. Midshaft cross-sectional bone geometry versus body mass for the emu Tbt. Cross-sectional area (*A*), C-C and M-L second moments of area (*B*; *I*), and polar moment of inertia (*C*) of the emu Tbt at the midshaft plotted against body mass on logarithmic axes. C-C (I_{CC}) and M-L (I_{ML}) data are represented by closed and open symbols, respectively. *A*, $y = 27.3x^{0.62 \pm 0.07}$ ($r^2 = 0.98$). *B*, I_{CC}: $y = 81.6x^{1.38 \pm 0.12}$ ($r^2 = 0.99$); I_{ML}: $y = 94.4x^{1.42 \pm 0.10}$ ($r^2 = 0.99$). *C*, $y = 176.0x^{1.40 \pm 0.11}$ ($r^2 = 0.99$). The dashed lines represent isometry in each case (slope: *A*, 0.67; *B*, *C*, 1.33), while the dotted lines represent the expected scaling relationships for the maintenance of static strain similarity (slope: *A*, 1.00; *B*, *C*, 1.67). These lines are positioned, starting from the origin, to facilitate comparison with the regression lines (*solid lines*).

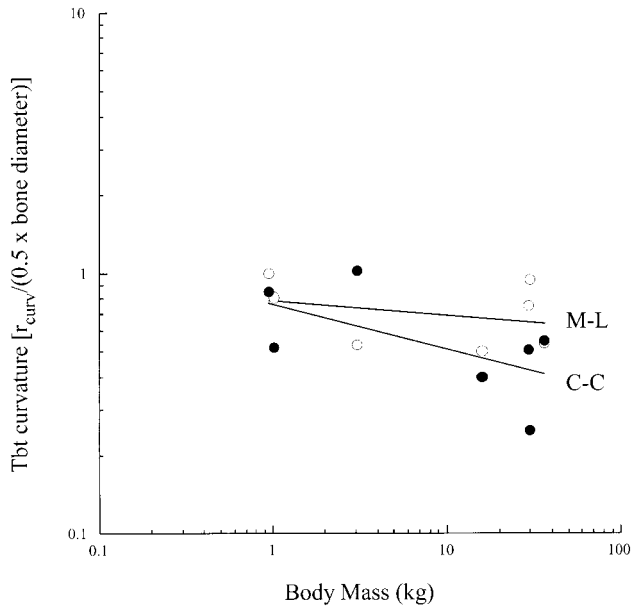

Figure 10. Normalized longitudinal bone curvature versus body mass in the emu Tbt. C-C and M-L longitudinal curvature of the emu Tbt plotted against body mass on logarithmic axes. C-C and M-L data are represented by closed and open symbols, respectively. C-C: $y = 0.76x^{-0.17\pm0.26}$ ($r^2 = 0.34$); M-L: $y = 0.79x^{-0.06\pm0.19}$ ($r^2 = 0.12$).

strains through ontogeny (Main and Biewener 2004). Although we observed a significant 2.8% increase in percent mineral ash content through ontogeny, it was not great enough to overcome the strong negative allometry in the cross-sectional geometry needed to maintain strains at similar levels through ontogeny.

Similar to the goats, peak limb loads on the emu hindlimb did not change significantly with an ontogenetic increase in body mass. Consequently, inherent features of the limb skeleton also likely explain the observed increase in strain within the emu Tbt. Although changes in bone mineralization have yet to be examined, ontogenetic scaling patterns of bone geometry and curvature adequately explain the general increase in strains in the emu Tbt during growth. The bone's cross-sectional area, second moments of area, and polar moment of inertia scale with isometry. Although not as far a departure as the negative allometry in the goat radius, this is still significantly below the scaling relationships required for static strain similarity (Fig. 9; $A\alpha M^{1.0}$, $I\alpha M^{1.67}$, $J\alpha M^{1.67}$), assuming that bone loads parallel patterns of limb ground reaction loading. Isometric growth of the bone coupled with little change in bone curvature through ontogeny could explain why growth-related increases in strain in the emu Tbt are less than those in the goat radius.

Changes in Safety Factor through Ontogeny

Just as the elastic modulus, *E*, increases through ontogeny, the same would be expected of the yield and ultimate strength of the bones (Currey and Butler 1975; Torzilli et al. 1981; Brear et al. 1990). A number of studies, typically from mammals, have examined how both the elastic modulus and ultimate breaking strains change through growth. For various mammals and one altricial bird (seagull), *E* has been found to increase between 1.3 and 5.3 times during ontogeny in mammals ranging from fetal or juvenile animals to adults (Currey and Butler 1975; Lanyon et al. 1979; Carrier 1983; Currey and Pond 1989; Brear et al. 1990) and 23 times in the California seagull (Carrier and Leon 1990) from prefledgling juveniles to adults. Similarly, breaking strengths (stresses) also increased. Breaking strains, however, decreased by about 1.3–2.3 times during ontogeny in the mammals and 3.6 times in the sea gulls. Because the values for the ontogenetic trends in *E* and breaking strains for birds are derived from a single species of altricial bird (seagull), whereas emu are precocial, walking within hours after hatching, the values for ontogenetic increases in bone strength for the generally precocial mammal species examined will also be applied to the emu in the following discussion interpreting ontogenetic changes in bone material properties in relation to in vivo bone strains. Although not ideal, this broad application of mammalian ontogenetic changes in material properties to the emu is a best estimate, given the paucity of data for ontogenetic changes in avian bone material properties from other precocial birds.

Although we did not conduct the appropriate mechanical tests to determine the material properties for the bones from the animals we examined, knowing how functional strains increase in goats and emu and breaking strains decrease in mammals through ontogeny, it is possible to estimate how safety factors may change during growth in goats and emu ([increase in locomotor strain × decrease in breaking strain]$^{-1}$ × 100). For example, because strains on the CR surface of the goat radius increase by 2.7 times and ultimate breaking strains in mammals decrease between 1.3 and 2.3 times during ontogeny, safety factors in the radii of adult goats are estimated to be between 16%–28% of those in young goats at a gallop, while in running emu, safety factors in the Tbt of a 48-wk-old, 26-kg bird would be between 17% and 31% of those in a 2-wk-old, 1-kg bird. Even if in vivo bone strains remained constant across size/age, safety factors in the bones of the adults would be at best only 43%–77% of those in the young animals, given the significant ontogenetic decrease in ultimate breaking strains.

Given the imprecision of these calculations, the predicted ranges are somewhat large. However, they indicate that for at least these two taxa, safety factors are not maintained similarly during growth but probably decrease as these animals increase in size and mass through ontogeny.

The Role of Selection and Behavior in Determining Ontogenetic Growth and Strain Patterns

Although safety factors likely decrease through ontogeny when comparing locomotor strains at similar relative speeds, com-

parisons at similar absolute speeds may be ecologically more relevant. For example, in predator/prey interactions in nature, it is not sufficient for a smaller prey animal to trot if the larger predator is trotting. The larger animal, cycling its legs at the same frequency as the smaller one, will achieve a faster absolute speed than the smaller animal by virtue of its longer stride length. Thus, it is necessary that smaller prey move at the same or faster absolute speed to escape predation. These speeds are achieved in smaller animals by using faster gaits characterized by higher limb loads and higher stride frequencies. However, at these speeds, they must still maintain a sufficiently high safety factor within the musculoskeletal system so as not to risk significant damage to the structures responsible for support and locomotion.

Goats are precocial animals that live in herds that include both adult and juvenile individuals. The movements of the herd, whether in response to predator threat or in search of food and water, require that younger animals with shorter legs maintain a relatively faster speed to keep pace with the adults. For example, to move at about 2.30 m/s, small goats gallop whereas adult goats trot. At these gaits, the limbs of the small and adult goats experience limb loads of about 1.7 BW and 1.2 BW while cycling their limbs at 3.23 and 2.37 strides per second, respectively. Thus, to keep up with adults moving at 2.30 m/s, the smaller goats must move at a relatively faster gait (gallop vs. trot) and incur significantly higher limb loads and a greater number of steps per second. However, on the basis of the peak strains measured and how the failure strain of mammalian bone generally changes with growth, the safety factor in the radius of these smaller animals is still about 4.4 times that of the adult goats, when both move at the same absolute speed.

Given that adult mammalian limb bones have similar ultimate breaking strengths of about -200 to -233 MN/m^2 (Biewener 1982) and that the stress in the radii of adult goats galloping is -41 MN/m^2 (Biewener 1991), the safety factor in the adult goat radius at a gallop is about 5, using ultimate breaking strength as the maximum strength of the bone. Thus, because young goats galloping have a safety factor between about three and six times that in adult goats at a gallop, they probably have a safety factor between about 15 and 30. However, these safety factors were determined using the ultimate breaking strength of mammalian bone, not the yield strength, which is more biologically relevant and which is typically 40% of ultimate strength (Rubin and Lanyon 1982; Biewener 1993), resulting in safety factors between 6 and 12 in the radii of galloping young goats.

Peak compressive strains in the adult radius ($-1{,}850$ $\mu\varepsilon$; Biewener and Taylor 1986) are within the range reported for most other vertebrates measured to date, which usually range between $-1{,}800$ $\mu\varepsilon$ and $-3{,}000$ $\mu\varepsilon$ (Rubin and Lanyon 1982). Thus, the negative growth allometry in the radius does not result in strains in the radii of the adult goats that are unusually high. This indicates that the radii of adult goats are not underbuilt but, rather, that those of the young goats are overbuilt, resulting in higher safety factors than have generally been observed in most adult vertebrates to date (Alexander 1981; Biewener 1982; Rubin and Lanyon 1982; Biewener and Dial 1995). So although young goats must move at a relatively faster speed to keep up with the herd and escape threats, they can do so while maintaining similar, if not higher, safety factors than adult goats moving at similar absolute speeds because of their relatively more robust limb bones.

Because the 30-fold increase in size examined in the emu is much greater than that in the goats (sevenfold increase), it is not possible to compare strains at the higher absolute speeds used by large birds during running because similar absolute speeds could not be attained by the much smaller birds. As a result, ontogenetic patterns of strain at similar absolute speeds for the emu were made at about 1.07 m/s, which corresponded to a fast walk or a slow run (DF 0.61) for "small" birds under 5 kg and to a slow walk (DF 0.69) for "large" birds more than 20 kg. In the emu, this speed may be more ecologically relevant than would be a faster speed because it better approximates the speeds used during foraging (0.3–1.1 m/s) or migration to water (1.4–2.0 m/s; Dawson et al. 1984), activities that would be performed by adult males and their broods. Predator or threat avoidance, which would typically require fast speeds and high limb loads in young animals, is very different in emu family groups than in herds of goats. When threatened, an adult male guarding his brood will give a warning call. In response to this call, the chicks drop and lay motionless (Gaukrodger 1925) or run quickly to the male (Fleay 1936), relying on his protection or their cryptic coloration and stillness to escape predation. Thus, it is perhaps the speed necessary to keep up with the flock during foraging that is a more important performance parameter for young growing emu than escape velocity and active predator avoidance.

At about 1.07 m/s, there was no significant difference in strains in the Tbt between the "small" and "large" emu, although mean peak Tbt strains in the "small" birds at this speed were somewhat lower. At this speed, even though the small birds are nearly running and incur higher relative limb loads at a higher frequency, they are able to maintain comparable, if not somewhat lower, strains than the "large" birds moving at a relatively slower speed.

Although the strains in the "small" birds are not two to three times lower than those in the "large" emu, as was the case in the goats when compared at similar absolute speeds, the young birds moving at relatively faster speeds are probably still able to maintain similar safety factors compared with the adults. The reason the emu do not show as large a difference in strain, and thus ontogenetic change in safety factor, as the goats is likely the result of isometric growth of the Tbt's cross-sectional geometry. Although isometric growth still favors an increase in peak strain through ontogeny, the increase is not as great as

the ontogenetic increase in strain in the goats that results from the strong negative allometry of the radius. Thus, the reason for the difference in the degree of bone strain increase through ontogeny between these two taxa is the result of young goats being more overbuilt relative to adult goats as compared with "small" versus "large" emu.

Why are young goats more overbuilt than young emu? This question presents an opportunity to investigate the relationship between growth strategies and natural histories in these two precocial taxa. Assuming that predator avoidance, more than acquiring food and mates, is the strongest selection pressure on locomotor performance in young precocial vertebrates, it is apparent why the limb bones examined reveal different growth strategies in these two taxa. Goats employ a very active form of predator avoidance, in contrast to the more passive form of predator avoidance displayed by young emu, which, when compared with the goats, could result in much weaker selection for a robust juvenile skeleton.

However, both the young goats and emu generally exhibit lower strains than the adults, indicating a greater resistance to similar, if not somewhat higher, relative loads in the limbs of younger animals at similar absolute speeds. This may additionally provide younger animals a greater safety factor during their early days when their movements may be less well coordinated, possibly resulting in more variable patterns of bone loading. With growth, the need for a higher safety factor would diminish as juvenile animals become more adept at walking and running. At this stage, the cost of maintaining relatively more robust limb bones may outweigh the risk of mechanical failure in the bones, which become loaded in a more predictable way as the animals grow and mature.

Life-History Strategies and Performance through Ontogeny in Vertebrates

The results of these studies partially agree with previous studies that have examined the relationships between ontogenetic changes in locomotor performance and musculoskeletal growth patterns in precocial animals. Similar to the patterns in the goat radius, black-tailed jackrabbits (*Lepus californicus*) show negative allometry in the second moment of area of the third metatarsal during ontogeny ($I \alpha M^{0.95 \pm 0.07}$; Carrier 1983). This produces relatively lower stresses in the bones of younger rabbits, which are less well mineralized and not as stiff as the bones of older rabbits (Carrier 1983). Carrier proposed that negative allometry in the metatarsal bone geometry, coupled with appropriate changes in the moment and contractile properties of the gastrocnemius, allowed younger and older rabbits a similar capacity for accelerating and escape velocity through ontogeny. Carrier and Leon (1990) further proposed that active young mammals and birds would generally show negative ontogenetic allometry in their limb bones to maintain high enough safety factors to compensate for immature, weak skeletal tissue in young animals. Although this seems to be true for young precocial mammals, precocial birds (emu and chickens; Biewener et al. 1986) show more variability in this pattern.

Two related studies examined bone strains (Biewener et al. 1986) and morphological scaling patterns in the chicken (*Gallus gallus*) Tbt during ontogenetic growth (Biewener and Bertram 1994) and found that the Tbt generally showed negative ontogenetic allometry in both cross-sectional ($A \alpha M^{0.55 \pm 0.07}$) and the C-C second moment of area ($I \alpha M^{1.22 \pm 0.12}$). Peak bone strains remained similar between 4- and 17-wk-old chickens at the same relative speeds (0.48 and 1.17 m/s, respectively), as measured by stride frequency and as a percent of maximum speed. However, this suggests that if young chicks approached the absolute speeds of adults, bone strains would exceed adult strain levels despite the chicks having relatively more robust tibiotarsi. These results contrast the similar or lower peak bone strains at similar absolute levels of locomotor performance observed in emu and goats.

Because Biewener et al. (1986) did not measure GRFs, it is difficult to assess why strains would be higher in younger animals traveling at similar absolute speeds as adults. The observations suggest that older chickens experience lower relative limb loads at functionally and absolutely equivalent speeds. However, the definition of equivalent relative speed differed between the earlier chicken study (stride frequency and 35% maximum speed) and the present studies (DF). Whether similar DFs correspond to similar stride frequencies as animals grow in size is equivocal, since stride frequencies at similar relative speeds did not change significantly in goats but decreased in the emu as the birds grew. If stride frequencies change through ontogeny in the chicken as they did in the emu, young chickens would have higher DFs (slower relative speed) than older chickens when moving at the same stride frequency. This suggests that if strains in the chicken Tbt were compared at similar DFs through ontogeny, younger chickens would still experience higher, rather than lower, strains in their Tbt.

In conclusion, it is possible to make some preliminary observations on the basis of this and previous studies examining the relationships between ontogenetic patterns in locomotor performance and musculoskeletal growth. First, even though taxa may show similar patterns of ontogenetic bone growth, different ontogenetic patterns of bone strain may result (e.g., chickens and goats). Second, except for the chickens, ontogenetic bone growth patterns correlate well with changing mechanical demands during locomotion in the life history of goats, jackrabbits, and emu. Lower strains and higher safety factors were observed in younger animals that are required to perform similarly to adults in particular situations, although they may not be as coordinated as the adults. Finally, the most drastic departures from the positive allometry expected to maintain strain similarity through growth in the limb bones occur in taxa where certain behaviors or performance characteristics are under strong selection in young animals (goats and rabbits).

Acknowledgments

We would like to thank the organizers of the symposium, Anthony Herrel and Alice Gibb. This work could not have been conducted without the assistance of Anna Ahn, Monica Daley, Colleen Donovan, Gary Gillis, Ty Hedrick, David Lee, Joyce Main, Craig McGowan, Polly McGuigan, Rebecca Mitchell, Ryan Monti, Pedro Ramirez, Stephanie Schur, and Jim Usherwood. Craig McGowan and two anonymous reviewers also provided valuable comments that improved the manuscript. This work was supported in part by the Chapman Fund (Harvard University).

Literature Cited

Alexander R.M. 1981. Factors of safety in the structure of animals. Sci Prog 67:109–130.

Alexander R.M. and A.S. Jayes. 1983. A dynamic similarity hypothesis for the gaits of quadrupedal mammals. J Zool (Lond) 201:135–152.

Alexander R.M., A.S. Jayes, G.M.O. Maloiy, and E.M. Wathuta. 1979. Allometry of the limb bones of mammals from shrews (*Sorex*) to elephant (*Loxodonta*). J Zool (Lond) 189:305–314.

Bertram J.E.A. and A.A. Biewener. 1992. Allometry and curvature in the long bones of quadrupedal mammals. J Zool (Lond) 226:455–467.

Biewener A.A. 1982. Bone strength in small mammals and bipedal birds: do safety factors change with body size? J Exp Biol 98:289–301.

———. 1983. Allometry of quadrupedal locomotion: the scaling of duty factor, bone curvature and limb orientation to body size. J Exp Biol 105:147–171.

———. 1989. Scaling body support in mammals: limb posture and muscle mechanics. Science 245:45–48.

———. 1991. Musculoskeletal design in relation to body size. J Biomech 24:19–29.

———. 1993. Safety factors in bone strength. Calcif Tissue Int 53:S68–S74.

Biewener A.A. and J.E.A. Bertram. 1994. Structural response of growing bone to exercise and disuse. J Appl Physiol 76: 946–955.

Biewener A.A. and K.P. Dial. 1995. In vivo strain in the humerus of pigeons (*Columba livia*) during flight. J Morphol 225:61–75.

Biewener A.A., S.M. Swartz, and J.E.A. Bertram. 1986. Bone modeling during growth: dynamic strain equilibrium in the chick tibiotarsus. Calcif Tissue Int 39:390–395.

Biewener A.A. and C.R. Taylor. 1986. Bone strain: a determinant of gait and speed? J Exp Biol 123:383–400.

Biewener A.A., J. Thomason, and L.E. Lanyon. 1983. Mechanics of locomotion in the forelimb of the horse (*Equus*): in vivo stress developed in the radius and metacarpus. J Zool (Lond) 201:67–82.

Blob R.W. and A.A. Biewener. 1999. In vivo locomotor strain in the hindlimb bones of *Alligator mississippiensis* and *Iguana iguana*: implications for the evolution of limb bone safety factor and non-sprawling limb posture. J Exp Biol 202:1023–1046.

Bradley N.S. and J.L. Smith. 1988. Neuromuscular patterns of stereotypic hindlimb behaviors in the first two postnatal months. I. Stepping in normal kittens. Dev Brain Res 38:37–52.

Brear K., J.D. Currey, and C.M. Pond. 1990. Ontogenetic changes in the mechanical properties of the femur of the polar bear *Ursus maritimus*. J Zool (Lond) 222:49–58.

Carrier D.R. 1983. Postnatal ontogeny of the musculo-skeletal system in the black-tailed jack rabbit (*Lepus californicus*). J Zool (Lond) 201:27–55.

Carrier D.R. and L.R. Leon. 1990. Skeletal growth and function in the California gull (*Larus californicus*). J Zool (Lond) 222: 375–389.

Carroll R.L. 1988. Vertebrate Paleontology and Evolution. W. H. Freeman, New York.

Cubo J. and A. Casinos. 1998. Biomechanical significance of cross-sectional geometry of avian long bones. Eur J Morphol 36:19–28.

Cubo J., L. Menten, and A. Casinos. 1999. Sagittal long bone curvature in birds. Ann Sci Nat Zool Biol Anim 20:153–159.

Currey J.D. 1987. The evolution of the mechanical properties of amniote bone. J Biomech 20:1035–1044.

———. 1999. What determines the bending strength of compact bone? J Exp Biol 202:2495–2503.

———. 2002. Bones: Structure and Mechanics. Princeton University Press, Princeton, NJ.

Currey J.D. and G. Butler. 1975. The mechanical properties of bone tissue in children. J Bone Jt Surg 57-A:810–814.

Currey J.D. and C.M. Pond. 1989. Mechanical properties of very young bone in the axis deer (*Axis axis*) and humans. J Zool (Lond) 218:59–67.

Dawson T.J., D. Read, E.M. Russell, and R.M. Herd. 1984. Seasonal variation in daily activity patterns, water relations and diet of emus. Emu 84:93–102.

Demes B., Y. Qin, J.T. Stern Jr., S.G. Larson, and C.T. Rubin. 2001. Patterns of strain in the macaque tibia during functional activity. Am J Phys Anthropol 116:257–265.

Erickson G.M., J. Catanese III, and T.M. Keaveny. 2002. Evolution of the biomechanical properties of the femur. Anat Rec 268:115–124.

Fleay D. 1936. Nesting of the emu. Emu 35:202–210.

Garland T., Jr. 1985. Ontogenetic and individual variation in size, shape and speed in the Australian agamid lizard *Amphibolurus nuchalis*. J Zool (Lond) 207:425–439.

Gatesy S.M. and A.A. Biewener. 1991. Bipedal locomotion: effects of speed, size and limb posture in birds and humans. J Zool (Lond) 224:127–147.

Gaukrodger D.W. 1925. The emu at home. Emu 25:53–57.

Heinrich R.E., C.B. Ruff, and J.Z. Adamczewski. 1999. Ontogenetic changes in mineralization and bone geometry in the femur of muskoxen (*Ovibos moschatus*). J Zool (Lond) 247: 215–223.

Hildebrand M. 1965. Symmetrical gaits of horses. Science 150: 701–708.

———. 1985. Walking and running. Pp. 38–57 in M. Hildebrand, D.M. Bramble, K.F. Liem, and D.B. Wake, eds. Functional Vertebrate Morphology. Harvard University Press, Cambridge, MA.

Irschick D.J. and B.C. Jayne. 2000. Size matters: ontogenetic variation in the three-dimensional kinematics of steady-speed locomotion in the lizard *Dipsosaurus dorsalis*. J Exp Biol 203:2133–2148.

Lanyon L.E., P.T. Magee, and D.G. Baggott. 1979. The relationship of functional stress and strain to the processes of bone remodelling: an experimental study on the sheep radius. J Biomech 12:593–600.

Main R.P. and A.A. Biewener. 2004. Ontogenetic patterns of limb loading, in vivo bone strains and growth in the goat radius. J Exp Biol 207:2577–2588.

Maloiy G.M.O., R.M. Alexander, R. Njau, and A.S. Jayes. 1979. Allometry of the legs of running birds. J Zool (Lond) 187: 161–167.

Muir G.D. 2000. Early ontogeny of locomotor behaviour: a comparison between altricial and precocial animals. Brain Res Bull 53:719–726.

Polk J.D., B. Demes, W.L. Jungers, A.R. Biknevicius, R.E. Heinrich, and J.A. Runestad. 2000. A comparison of primate, carnivoran and rodent limb bone cross-sectional properties: are primates really unique? J Hum Evol 39:297–325.

Rubenson J., D.B. Heliams, D.G. Lloyd, and P.A. Fournier. 2004. Gait selection in the ostrich: mechanical and metabolic characteristics of walking and running with and without an aerial phase. Proc R Soc Lond B 271:1091–1099.

Rubin C.T. and L.E. Lanyon. 1982. Limb mechanics as a function of speed and gait: a study of functional strains in the radius and tibia of horse and dog. J Exp Biol 101:187–211.

Selker F. and D.R. Carter. 1989. Scaling of long bone fracture strength with animal mass. J Biomech 22:1175–1183.

Torzilli P.A., K. Takebe, A.H. Burstein, and K.G. Heiple. 1981. Structural properties of immature canine bone. J Biomech Eng 103:232–238.